

Research Paper

Mixed Matrix Membranes from Polyvinylchloride and Manganese Organic Complex Compound for Fouling and Viral Resistance

Heba Abdallah Mohamed Abdallah ^{1,*}, Marwa Saied Shalaby ¹, Li-Feng Fang ², Bao-Ku Zhu ², Ahmed Mahmoud Shaban ³¹ Chemical Engineering and Pilot Plant Department, Engineering Research Division, National Research Centre, El-Bohouth St. (Former El-Tahrir St.), Dokki, Giza, PO box 12622, Affiliation ID: 60014618, Egypt² Department of Polymer Science and Engineering, ERC of Membrane and Water Treatment (MOC), Key Laboratory of Macromolecular Synthesis and Functionalization (MOE), Zhejiang University, Hangzhou 310027, China³ Water Pollution Research Department, Environmental Research Division, National Research Centre El-Bohouth St. (Former El-Tahrir St.), Dokki, Giza, PO box 12622, Affiliation ID: 6001461, Egypt

Article info

Received 2020-07-19

Revised 2020-09-16

Accepted 2020-09-25

Available online 2020-09-25

Keywords

Manganese acetylacetonate
 Polyvinylchloride
 Mixed matrix membranes (MMMs)
 Antifouling
 Viral Resistance

Highlights

- Mn(acac)₃ were prepared by the green method
- Mixed matrix membranes from PVC with Mn(acac)₃ were prepared
- Prepared membranes can resist fouling & viruses

Abstract

Fouling and virus resistance membranes were prepared by the blending of polyvinylchloride (PVC) with a solution (NS) of manganese acetylacetonate Mn(acac)₃. Mixed matrix membranes PVC/Mn(acac)₃ exhibit enhancement in properties and performance compared with the blank membrane. In a comparison among the fabricated mixed matrix membranes, U4 which was prepared from 14 wt% PVC with 1wt% nano-solution of Mn(acac)₃ exhibits the highest mechanical properties compared with the blank membrane and other prepared membrane samples of U3 (15% PVC & 1%NS), U5 (14% PVC & 0.5% NS), U6 (14% PVC & 0.2% NS), and U7 (14% PVC & 1.2% NS). The addition of Mn(acac)₃ nano-solution to polymeric solution improved the hydrophilicity of the membrane samples, where the blank membrane U1 (16% PVC) exhibited a contact angle of 127.1°±0.5° compared with 40.1°±0.1° for U7 and 48.5°±0.1° for U4. Moreover, the membranes' performance was improved, where U1 (blank) provided the permeate flux of 65, 51, 40, and 26 L/m².h and U4 provided 90, 86, 76, and 73 L/m².h for separation of various concentrations of humic acid 0.05, 0.1, 0.2, and 1 g/L, respectively. A virus removal test was carried out on real sewage wastewater. U4 provides 100% removal for all virus removal, while U1 provides 100% removal for rotavirus only. The fouling test results indicate that U4 exhibited antifouling properties, where the flux recovery ratio (FRR) was 99.47%. So, the mixed matrix membrane U4 can be considered as a fouling and virus resistance membrane.

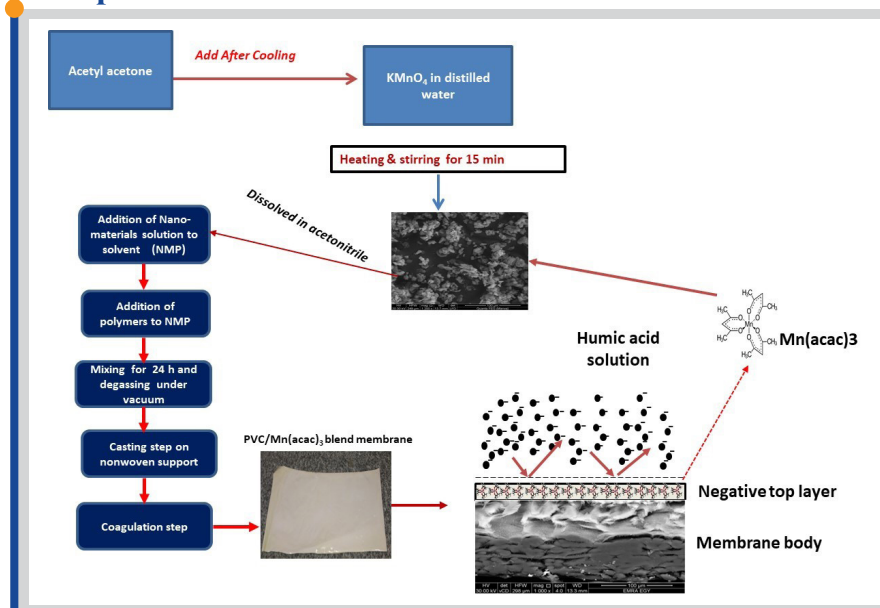
1. Introduction

Wastewater is one of the water sources that must be treated to be reused in agriculture irrigation, so it must have tertiary treatment to ensure that it is free from viruses that may affect human health. Ultrafiltration is a promising process for water treatment due to the high quality and quantity of produced

water under low-pressure operation, which was used to remove bacteria, viruses, organics, and suspended solids [1].

The most common polymeric materials that are used in ultrafiltration membranes preparation are polyvinylchloride (PVC), polyethylene (PE),

Graphical abstract



© 2021 MPRL. All rights reserved.

* Corresponding author: E-mail address: drhebaabdallah3@gmail.com (H.A.M. Abdallah)

polyvinylidene fluoride (PVDF), polysulfone (PS), and polyethersulfone (PES). The selection of these polymers depends on the nature of using and the backbone materials which can lead to provide the cost of the membranes [2,3]. Using polyvinylchloride (PVC) as the main polymer in the ultrafiltration membrane preparation improves the mechanical strength, physical and chemical properties like resistance to acids, bases, solvents, and chlorine [4-6]. However, the PVC is cheaper than PVDF, so it can be used to produce low-cost UF membranes [7-9].

Fouling of membrane leads to a decline in permeate flux, selectivity and reduces the lifetime of membranes during operation. The fouling can be divided into inorganic fouling, colloidal fouling, organic fouling, and biofouling [10]. According to the type of fouling, many modifications on membranes during preparation should be taken into consideration to prevent clogging [11-13]. However, additives that improve the hydrophilicity of membranes surface can also improve antifouling properties [14-17]. J. Cai et al. studied the addition of supramolecules such as polyamidoamine to the membrane surface through one step interfacial polymerization with piperazine, where the modified membranes exhibit high separation performance for monovalent and divalent anions because the surface of the membrane gains modified pore-size with surface charge [18].

Blending between two polymers or embedding with nano-materials are considered versatility and simplicity method [17-20]. El-Gendi et al. prepared membranes by blending between polyvinyl chloride and cellulose acetate provide good membrane performance for desalination, where the different concentration of the salty solution was applied in desalination test using different grades of blend membranes from polyvinyl chloride and cellulose acetate, where the results indicated high membranes performance according to high rejection percentage over 90% and good permeate flux [21].

Inorganic-polymer composite membranes can be prepared using different nanoparticles like alumina (Al_2O_3) [22], titanium dioxide (TiO_2) [23,24], zirconium (ZrO_2) [25], silica (SiO_2) [26] and multi-walled carbon nanotubes (MWCNTs) [27,28].

Manganese complexes compounds were used to attack the viruses' protein layer, so many researches were studied the effectiveness of manages complexes compounds in viruses and organics removal [29,30]. For example, Nonstoichiometric perovskite-type $LaxMnO_3$ has been used as disinfection for influenza (A) virus, which can oxidize the residues of amino acids in the envelope of proteins in influenza viruses, neuraminidase, and hemagglutinin, that leads to deactivation for the cover of protein, then neutralize the virus [31,32].

Metal-organic complexes have high dispersion degree due to a hydrogen bond between them and the membrane materials. Also, according to coordination between metal ions and organic molecules, which can perform one, two- or three-dimensional structure, these materials have high porosity and high surface area [33,34]. Using these materials during membrane preparation lead to improve membrane performance, the hydrophilicity, strength, stiffness, water permeability, and antifouling properties [33,34].

Manganese acetylacetonates $Mn(acac)_3$ was used as a novel material in membrane preparation, mostly it was used as a catalyst in polymerization and isomerization reaction industries, so this material can enhance the polymerization process of polymeric solutions during preparation. Manganese acetylacetonates $Mn(acac)_3$ are coordination complexes that have a tetragonal structure, according to coordination between metal ions and organic molecules, which can perform one, two- or three-dimensional structure, these materials have high porosity and high surface area [33, 34]. Using these materials during membrane preparation lead to improve the membrane performance, the hydrophilicity, strength, stiffness, water permeability, and antifouling properties [33-36].

The novelty of this work is to use low-cost polymeric materials such as PVC, where it is used in the many industrial applications to produce different plastic products, so it is widely used in plastic industries due to its low cost. Ultrafiltration membranes modules have high prices according to that using low-cost polymers can reduce the price of UF membranes production. Alsahy et al. studied the preparation of PVC hollow fiber membranes to be used as an ultrafiltration membrane to separate polyvinylpyrrolidone from the water, where the rejection reached 97.5% at using PVC concentration 19wt% [37]. Jin et al. studied the preparation of blend polyvinylchloride with diphenyl ketone in blending solvents N, N-dimethylacetamide/N, N-dimethylformamide to produce ultrafiltration membranes were used for separation of bovine serum albumin (BSA) with a molecular weight of 67 kDa, where the separation percentage reached 85% at PVC concentration of 16 wt% [38]. Krishnamoorthy et al. studied the preparation of blend PVC with cellulose acetate to fabricate the ultrafiltration membrane for protein removal, where the rejection reached 72 % for pepsin, 65% for trypsin at using blending ratio equal 9 of (CA/PVC) [39]. Also, the novelty of this work was the development membranes to improve the resistance of fouling and virus using metal acetylacetonates like $Mn(acac)_3$, where the geometric shape

and negative charge of $Mn(acac)_3$ can improve the membrane performance in terms of permeability and removal percentage as well as provides a benefit from the charge of the metal to improve the membrane surface to resist the fouling and resist any viruses to pass through the membrane.

In this work blending between polyvinylchloride and manganese acetylacetonate as one of metal acetylacetonate complexes was studied due to the advantages of $Mn(acac)_3$ which has a high surface area structure that leading to improve prepared membranes properties. The prepared membranes were characterized by SEM, FTIR, mechanical properties, and contact angle. Finally, the performance of the membranes was investigated using prepared samples from synthetic humic acid solution and real sewage wastewater to test the fouling and virus resistance.

2. Experimental work

2.1. Materials

Polyvinylchloride (PVC) was purchased from Roth India Company. It was used as the main polymer, which was blended with nano-solution that was prepared by Manganese acetylacetonate $Mn(acac)_3$ and acetonitrile. Acetonitrile was purchased from Sigma Aldrich. N-methyl-2- pyrrolidone (NMP) was used as a solvent and polyethylene glycol (PEG 400) was used as a pore former additive, both were purchased from Fluka. Technical grade acetylacetone was purchased from Fluka and potassium permanganate ($KMnO_4$) was obtained from Sigma-Aldrich.

2.2. Synthesis of nano-particles preparation $Mn(acac)_3$

Manganese acetylacetonate $Mn(acac)_3$ was synthesized by dissolving five grams of potassium permanganate in 50 mL of deionized water. The mixture was stirred continuously, then acetylacetone was added to the solution. The mixture was left to cool for 10 min for complete precipitation of dark shiny crystals of $Mn(acac)_3$, then the powder was dried in a vacuum oven for 15 min [40]. Zeta potential analysis of nano-particles was studied under different pH 2, 3, 5, 7, and 8 using system Santa Barbara, Calif, USA.

2.2.1. Characterization of Nanoparticle by Scan Electron Microscopy and XRD

The powder samples SEM was performed using a JEOL 5410 scanning electron microscope at 20 kV. XRD analysis for powder samples was carried out by the XRD spectrum (Bruker 8 advance, CuK, target with secondary monochromator $\lambda = 40$, mA = 40, Germany), where the XRD patterns were determined at room temperature using an X-ray generator (Shimadzu XDD1, Japan).

2.3. Membranes preparation

Polyvinylchloride (PVC)/ Manganese acetylacetonate $Mn(acac)_3$ membranes were prepared using the phase inversion technique. The polymer PVC was dissolved in a solvent (NMP) with $Mn(acac)_3$ solution. $Mn(acac)_3$ solution was prepared by mixing 1g of $Mn(acac)_3$ with 10 gm acetonitrile and mixing for 30 min by mechanical stirrer under sonication, the solution of $Mn(acac)_3$ in acetonitrile is called nano-solution (NS). Then a different percentage of these solutions was studied in the polymeric mixture. The polymeric mixture was stirred under room temperature 25°C for 24h. The percentages of polymeric solutions were depicted in Table 1. The casting solution was drawn onto a non-woven fabric.

Table 1
Polymeric Solution Composition for PVC/ $Mn(acac)_3$ membranes.

Membrane Symbol	Composition (Weight Percentage)			
	PVC %	PEG%	NMP %	NS %
U1	16	0	84	0
U2	14	2	84	0
U3	15	2	82	1
U4	14	3	82	1
U5	14	3	82.5	0.5
U6	14	3	82.8	0.2
U7	14	3	81.8	1.2

2.4. Membrane characterization

2.4.1. Scanning electron microscope

A scanning electron microscope (SEM) was carried out by a JEOL 5410 scanning electron microscope apparatus on the membrane's surface and cross-sections. The samples were coated with gold to supply electrical conductivity. The images were conducted at 30 kV.

2.4.2. Mechanical test

Mechanical properties of membranes samples were performed using a mechanical testing system H5KS universal testing machine. The sample dimensions were 10 cm in length and 2.5 cm in width. The tensile strength and elongation were measured at a rate of 5 cm/ min for all samples. An average of three samples for all prepared membranes were recorded.

2.4.3. Porosity measurements

The porosity of membranes was measured using densometer device, the sample area is 25 cm², and the mechanism of the device depends on recording the flow of the air by measuring the time of the flow at a given volume of air through the membrane pores. The air pressure was applied using an inner cylinder has a specific diameter, which is float freely over the outer cylinder partly filled with oil which acts as an air seal. The air permeability of membranes samples and the porosity was calculated using equation (1) and (2) [41].

$$P = \frac{135.5}{t} \tag{1}$$

$$\emptyset = \frac{PC}{r^2} \tag{2}$$

where:

P: Air permeability ml/(cm².s.psi)

t: time in seconds

r: Radius of the device circular ring, where, r²=6.25 cm²

C: constant (equals 2 for the circular device rings).

∅: Membrane porosity

2.4.4. Contact angle measurements

Membranes samples contact angles by sessile drop method were measured by a compact video microscope (CVM) that was operated

according to the standard test method (ASTM D724-99) of the surface wettability of paper and standard methods (ASTM D5946- 96) of corona-treated polymer films [41]. The volume of droplets on samples was 10μL, where the photo was taken directly after the addition of every drop. An average of three measurements was recorded.

2.4.5. Fourier transform infrared (FTIR) spectrophotometer

FTIR analysis at a resolution of 4 cm⁻¹ with 16 scans/min was carried out on membranes samples (U1 & U4) using apparatus JASCO FT-IR 6100. The IR data were determined in the wavenumber range from 400 to 4000 cm⁻¹.

2.5. Membrane performance

A laboratory-scale filtration system is composed of a feeding tank. It was fixed on a hotplate for mixing, pump, pressure regulator, and dead-end membrane cell. This system was used to indicate the efficiency of the prepared membranes as shown in Figure 1. The effective area of the membrane in the test cell was 13.86 cm². Different Humic acid solutions concentrations (0.05, 0.1, 0.2, and 1 g/l) were fed at a fixed feed pressure (2 bar) to determine the prepared membranes' performance at room temperature. The feed and produced treated water were analyzed by UV analysis. Real sewage wastewater after secondary treatment from Zenin wastewater treatment station in Giza, Egypt was used to indicate the effectiveness of virus separation by the membranes, the water samples were analyzed by Polymerase chain reaction analyzer (PCR) before and after membrane.

2.6. Membrane fouling testing

This test was carried out using the same apparatus of the membrane performance test. The dead-end mode system was used because it exposes the membrane surface to the worst flow perpendicular on the membrane surface which can form clogging to the pores and make a cake layer on the surface which are considered the main reason for the fouling formation [42]. Humic acid solution 1 g/L was used in this test for 5h. It was performed on U1, U2, and U4. Pure water was fed first through membranes for 1h, where J_{w1} (L/m².h) was calculated. After that, a humic acid solution was fed to membranes for 2h. J_p (L/m².h) was determined. Pure water again was fed to membranes for 1 h and J_{w2} (L/m².h) was determined. The test was performed for 5 h. equation (3) was used to calculate the flux recovery ratio (FRR) [43, 44].

$$FRR \% = \frac{J_{w2}}{J_{w1}} \times 100 \tag{3}$$

Equation (4) was used to calculate total fouling resistance (R_f):

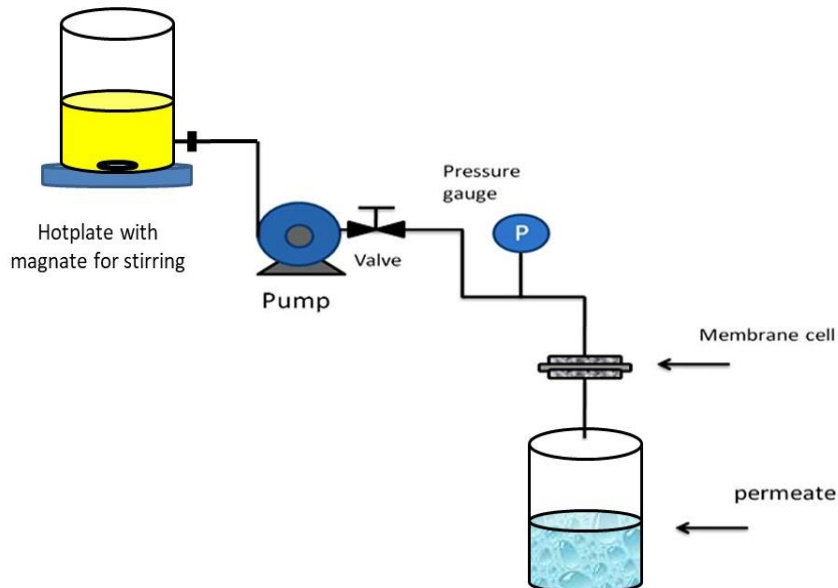


Fig.1. Schematic diagram of the filtration setup.

$$R_t \% = \left(1 - \frac{J_p}{J_w}\right) \times 100 \quad (4)$$

Equations (5) & (6) were used to calculate the irreversible fouling resistance (R_{ir}) reversible resistance [43,44].

$$R_r \% = \left(\frac{J_{w2} - J_p}{J_{w1}}\right) \times 100 \quad (5)$$

$$R_{ir} \% = \left(\frac{J_{w1} - J_{w2}}{J_{w1}}\right) \times 100 \quad (6)$$

Permeate flux J_i (w_1 & w_2) was calculated using equation [7]:

$$J = \frac{Q}{A \cdot t} \quad (7)$$

where Q is the volume of produced water after membrane which was collected in L ; A is the effective area of the membrane in m^2 and t is a time in hours.

3. Results and discussion

3.1. Nanoparticle characterization

3.1.1. Zeta Potential

Figure 2 indicates the results of zeta potential for $Mn(acac)_3$ nanoparticles, which were studied using different pH solutions 2, 3, 5, 7, and 8, the results indicate that at $pH = 7$, the zeta potential was -34.1 mV, while after increasing the pH to 8, the zeta potential was -38.2 mV. Also, reducing pH exhibits negative zeta potential, where it was -28 , -12 , and -2 at pH 5, 3, and 2 respectively. That means using $Mn(acac)_3$ in membrane preparation leads to a negative charge on the membrane surface. $Mn(acac)_3$ configuration has unpaired two electrons, so it provides paramagnetic behavior, which can provide electrostatic interactions between this nano-particle and the other particles in the medium. However, the negative charge means these nanoparticles have never been dissolved in water [45,46].

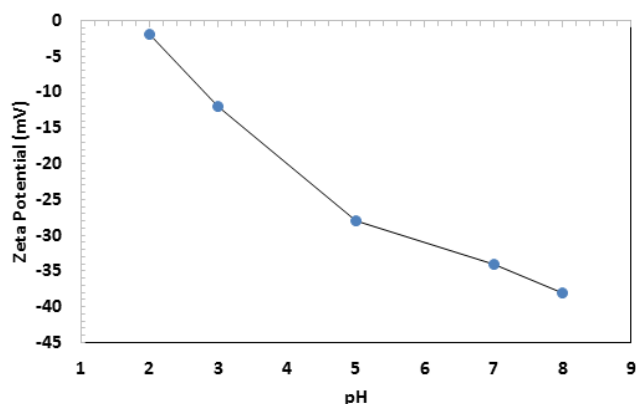


Fig. 2. Zeta potential as a function of pH for prepared $Mn(acac)_3$ nano-particles.

3.1.2. XRD & SEM for powder

Figure 3 explains XRD-spectrum which indicates nanoparticles amorphous state. The sharp peak with a purity of 100% ($d = 8.5609$) belongs to $Mn(acac)_3$. While other peaks appear to correspond to the associated organic impurities. The XRD results agreed with the published literature [40].

Figure 4 indicates SEM of the prepared powder with magnification power 80x and 1200x, this material was prepared using a homogenizer without using sophisticated sonication, so the SEM images indicate the formation of the crystalline aggregates' product. The particle clusters are not spherical, but they have an irregular shape. The size distribution of the nanoparticles is non-uniform due to the simple preparation method without the need for any calcination [40].

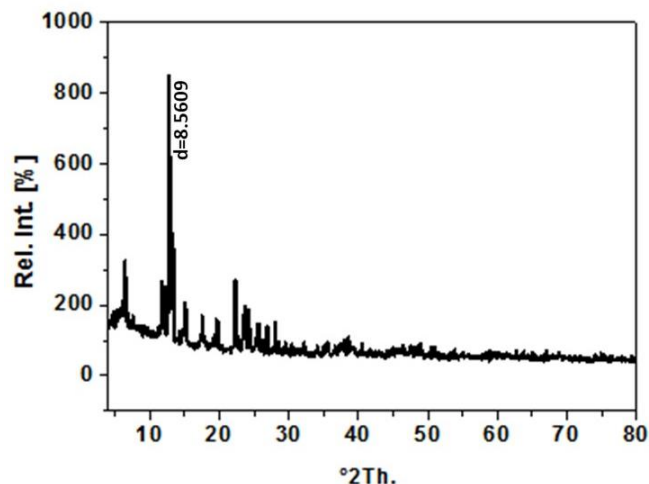


Fig. 3. XRD for $Mn(acac)_3$ powder.

3.2. Membranes characterization

3.2.1. Scanning electron microscopy

Different percentage of manganese acetylacetonate solution was added to the polymeric solution, to improve antifouling properties of membranes. Figure 5 illustrates that the U1, which represents a blank PVC membrane without any addition of nano-solution, exhibits a dense membrane top surface with a spongy membrane body structure. U2 represents a porous surface and the cross-section of the membrane exhibits a spongy structure. U2 membrane was prepared using polyethylene glycol (PEG 2wt%) as a pore former. U3 membrane was prepared using a high percentage of PVC (15wt%) and PEG 2wt% with $Mn(acac)_3$ solution 1wt%. U3 provides a dense membrane structure with reducing the finger-like structure due to high polymer concentration and using the nanoparticles solution, which leads to reduce the size of the pores. U4 membrane exhibits a wonderful structure, which consists of three layers top porous surface, wide finger-like shape with high tortuosity in the sub-layer, and porous bottom layer according to use the nonwoven support, this structure was due to using pore former PEG 3wt% and nano-solution 1wt% that can effect on the formation of finger-like size and shape [47]. U5 membrane also represents three layers in the cross-section of the membrane with a low size finger-like structure due to a decrease in the percentage of nano-solution to 0.5%. U6 membrane cross-section exhibits a spongy structure again due to reduce the percentage of nano-solution to 0.2 wt%. U7 membrane represents a wide and straight finger-like structure, also the top surface of the membrane is porous but less in pores size compared with U4 that due to using PEG 3% and $Mn(acac)_3$ nano-solution 1.2wt%. Using $Mn(acac)_3$ provides the membrane high surface area and high pore volume according to its tetragonal structure, where it forms three-dimensional matrix multi-connections with the polymer chains [36,48]. Polyethylene glycol is one of the common pore former additives, also it enhances the hydrophilicity of the surface and improves the diffusive transport properties of the water through the membrane surface. So, the selection of the PEG percentage should be determined according to the preliminary experiments, also the nonwoven support should be taken in our consideration because it is porous support, which leads to an increase the porosity of the membrane, so high concentration of PEG leads to increase in pores size. Increasing the percentage of PEG from 2 wt% to 3 wt% that because the addition of $Mn(acac)_3$ reduces the size of the pores of membranes, so to control the size of the pores and pores distribution in membrane surface, the percentage of PEG was increased to 3 wt% to adjust the pores size and membrane porosity [39, 49]. Increasing the percentage of $Mn(acac)_3$ nano- solution leads to aggregation of the $Mn(acac)_3$ nanoparticles and increasing the viscosity of the polymeric solution during preparation, which causes rapid liquid-liquid phase separation in the coagulation step during membrane formation, and that can form weak points on the body of the membrane, so the high percentage of nano solution of $Mn(acac)_3$ was adjusted to be 1.2wt%.

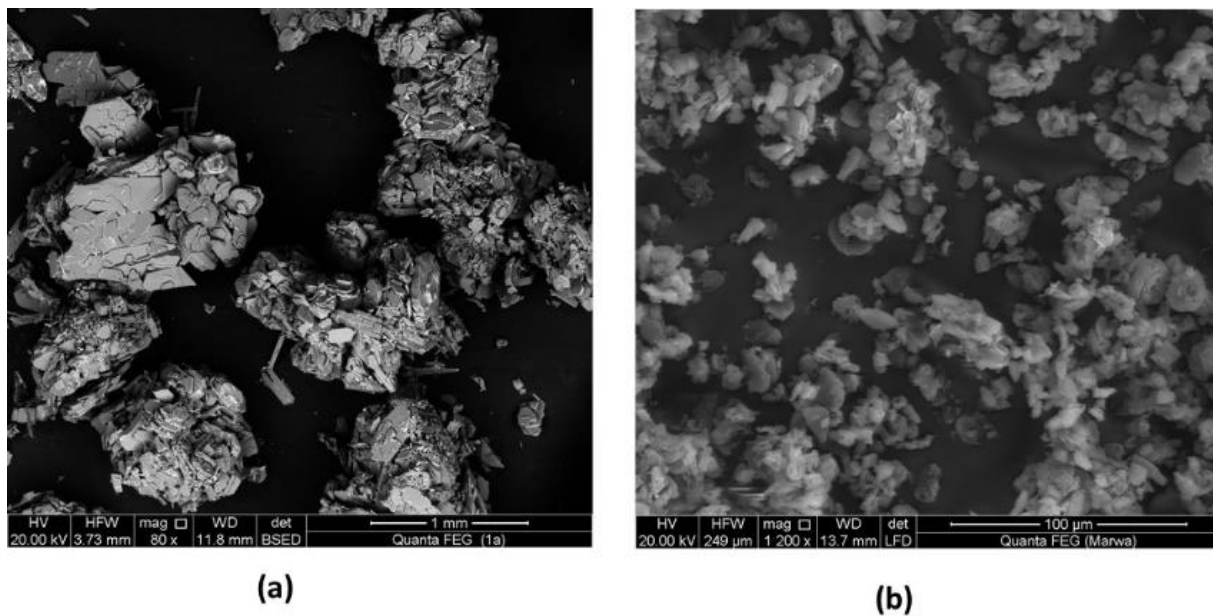


Fig. 4. SEM of Mn(acac)₃ Powder, where (a) at magnification power 80x and (b) at magnification power 1200x.

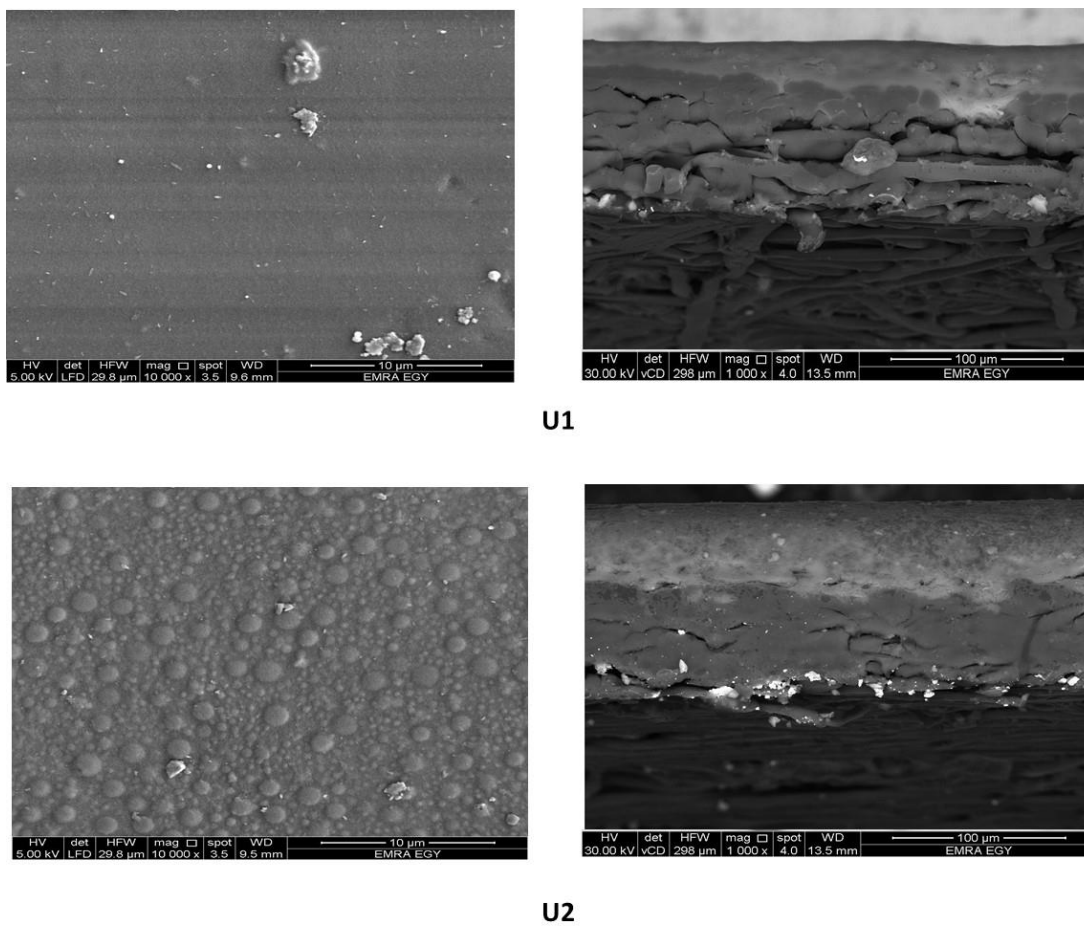
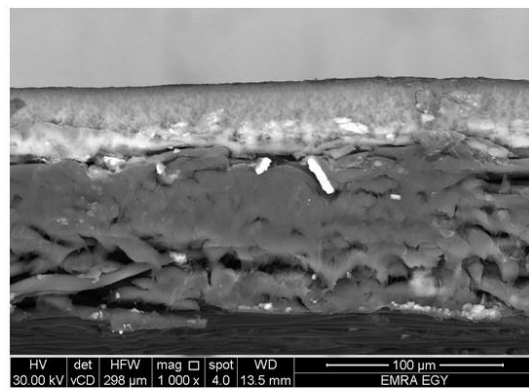
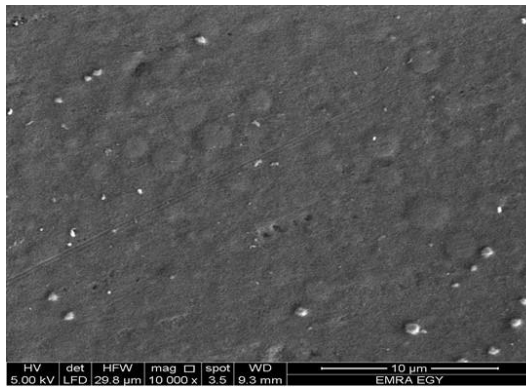
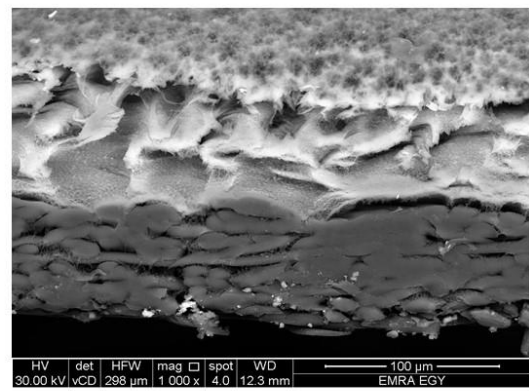
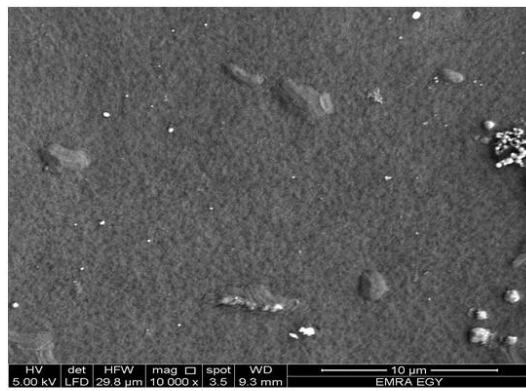


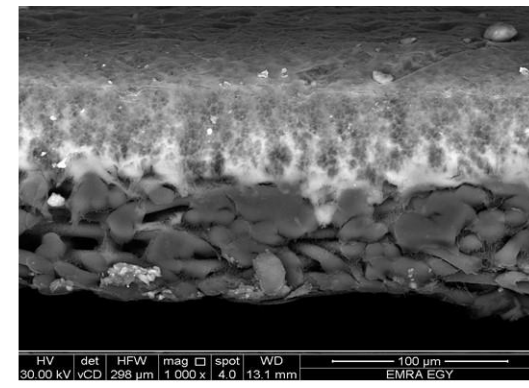
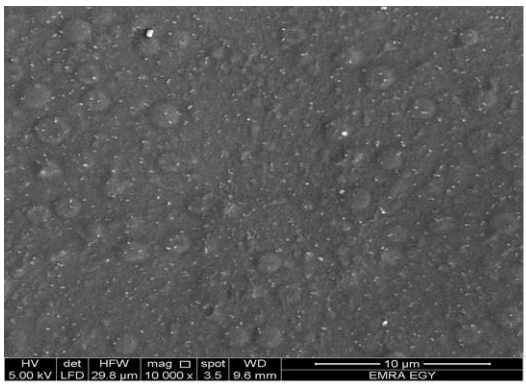
Fig. 5. SEM Photos for prepared membranes.



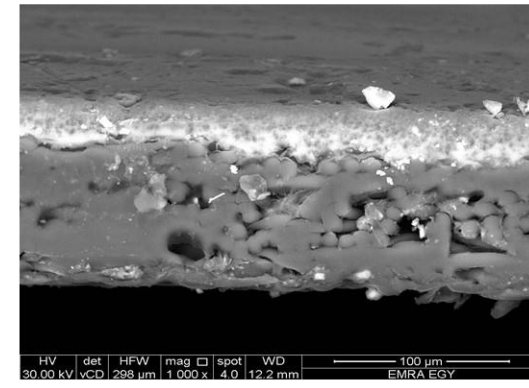
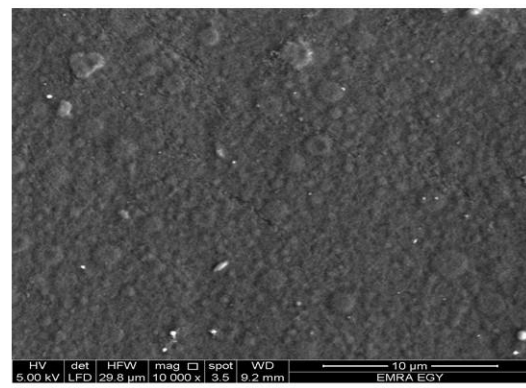
U3



U4

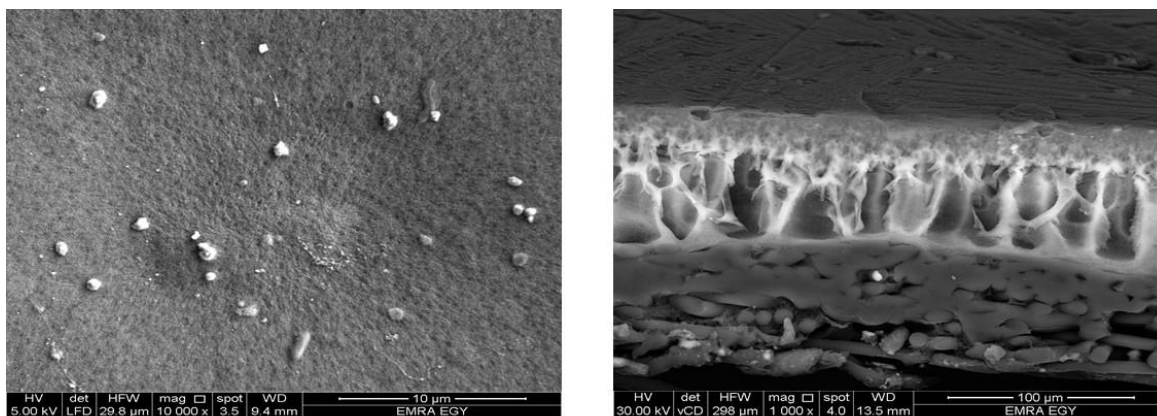


U5



U6

Fig. 5. Continued.



U7

Fig. 5. Continued.

3.2.2. Mechanical properties

Figure 6 illustrates the results of the mechanical test depending on the percentage of nano-solution of $Mn(acac)_3$; the results indicate that U4 provides the highest tensile strength of 221.7 ± 0.05 MPa, and elongation of $20.12 \pm 0.1\%$, while U3 has the lowest mechanical properties: tensile strength of 114.16 ± 0.05 MPa with elongation of $13 \pm 0.2\%$. The enhancement of the tensile strength of membranes is in the following sequence $U4 > U5 > U6 > U2 > U1 > U7 > U3$. According to Table 1, U4 which was prepared from PVC 14 wt%, PEG 3wt% with nano-solution 1wt% has the highest mechanical properties, which indicates the optimum addition of nano-solution for this polymeric solution is 1 wt%. The increase in the percentage of nano-solution, in this case, leads to an increase in the voids in the membrane leading to a reduction in tensile strength but improvement in elongation such as U7. The elongation enhancement of the membranes is in the following sequence $U4 > U7 > U5 > U6 > U2 > U1 > U3$. Improvement in elongation may be due to using acetonitrile in the nano-solution preparation, which improves the elasticity of the membranes, that because acetonitrile is used as a ligand in many transition metal complexes, which can be considered easily displaceable ligand [26,50]. The reduction in tensile strength at using 1.2 wt% NS in U7 preparation is related to the aggregation of nanoparticles which can cause stress assemblage points in the membrane body. The aggregation of nanoparticles during membrane formation can lead to interstitial defects,

which can affect membrane performance and lost some of its properties [51]. However, using polyester nonwoven support enhances the tensile strength of the membranes samples.

3.2.3. Porosity measurements and contact angle

Table 2 exhibits average porosity and contact angle measurement. The results indicate that U2 has the highest porosity of $56.2 \pm 0.2\%$ due to using pore former PEG without nanomaterials solution, while U7 has the lowest porosity of $48.6 \pm 0.2\%$ due to using a high percentage of nano-solution 1.2wt%. Increasing nano-solution of $Mn(acac)_3$ leads to a reduction in the size of the pores, which leads to a decrease in membrane porosity, however, the high dispersion degree of $Mn(acac)_3$ with H-bonding of polymers ligand substitution can lead to improvements in membranes pores distributions. The blank polyvinylchloride is a hydrophobic membrane, where the contact angle of U1 was $127.1^\circ \pm 0.5^\circ$. The addition of nano-solution of $Mn(acac)_3$ with acetonitrile increases the hydrophilicity according to the results in Table 2, where the contact angle decreased to $40.1^\circ \pm 0.1^\circ$ for U7 due to the addition of 1.2wt% of this solution. Acetonitrile in nano-solution forms a strong interaction between the polymer and $Mn(acac)_3$ that leading to a change in hydrophobicity, pore size, and free volume due to polymeric network chain rearrangement [42,47].

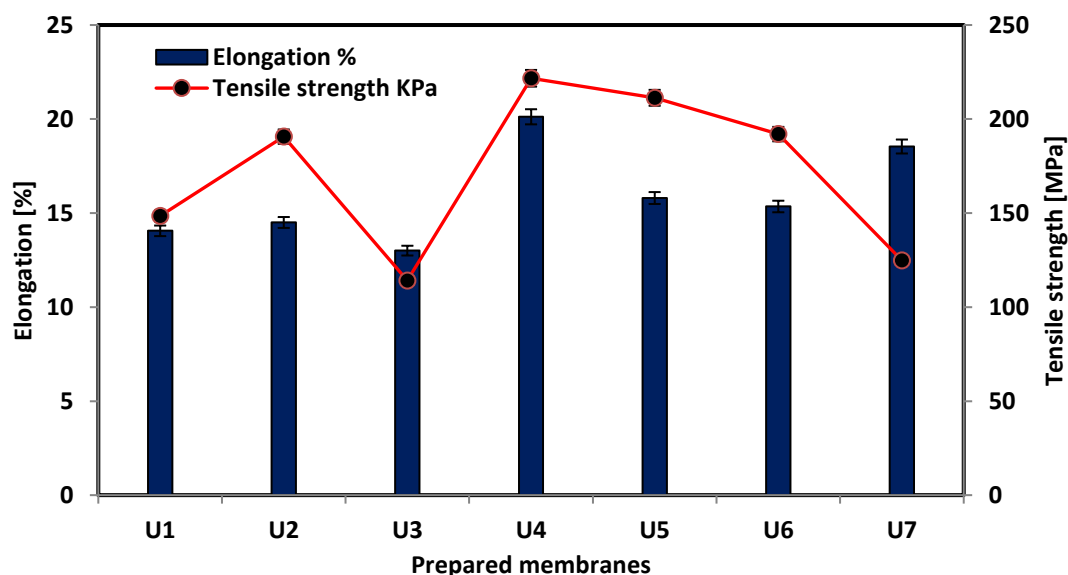
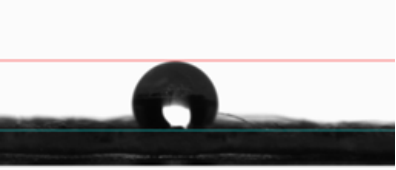
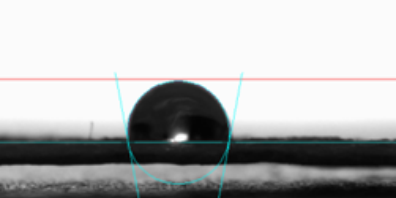
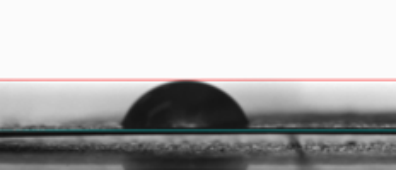
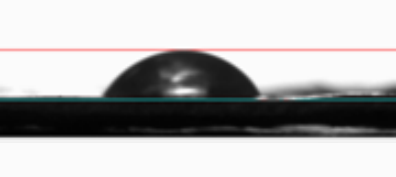
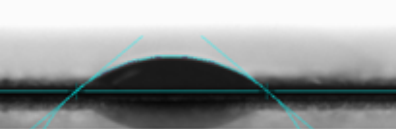


Fig. 6. Mechanical Properties of prepared UF (PVC/ $Mn(acac)_3$) membranes.

Table 2
Porosity and contact angle measurements of prepared membranes.

Membranes	Porosity %	Contact angle [°]	Wettability image
U1	54.3 ± 0.05	127.1 ± 0.5	
U2	56.2 ± 0.2	100.5 ± 0.2	
U3	52.3 ± 0.5	75.5 ± 0.4	
U4	50.2 ± 0.1	48.5 ± 0.6	
U5	53.4 ± 0.3	56.5 ± 0.2	
U6	55.4 ± 0.5	67.6 ± 0.5	
U7	48.6 ± 0.2	40.1 ± 0.1	

3.2.4. Fourier transform infrared (FTIR) spectrophotometer

Figure 7 indicates the IR spectrum of blank PVC (U1) and mixed matrix membrane U4; (14 % PVC/1 % sol Mn(acac)₃). PVC membrane (U1) sample indicates peaks in the region between 506 cm⁻¹ and 632 cm⁻¹ allocated to C-Cl stretching vibration. However, peaks vibration between 1960 cm⁻¹ to 2535 cm⁻¹ is related to asymmetric C-H stretching. The peaks at 722 cm⁻¹ to 943 cm⁻¹ are the indication for polyethyleneglycol observation in terms of group CH₂O and the peaks at 970 cm⁻¹ to 1064 cm⁻¹ correspond to the C-O stretching of C-O-C group of the PEG [49].

The coordination bond between the metal and acetylacetonate appears in the peaks 404 to 556 cm⁻¹. Asymmetric stretching of the carbonyl group in acetylacetonate appears in peaks from 1622 to 1800 cm⁻¹. A broad band was observed at 2966 to 3544 cm⁻¹ due to the formation of the -OH group in the matrix of the PVC membrane. Peaks between 1427.9 to 1500 cm⁻¹ indicate CH₂ scissors vibration band due to the crystalline component of PVC with the bonding of Mn(acac)₃ to form a matrix of PVC with Mn(acac)₃ in a complex

interaction [52]. The peaks from 1490 cm⁻¹ to 1580 cm⁻¹ is an indication of the attraction between polyester (PET) support and the membrane. The results of FTIR are shown in Table 3 [42].

3.3. Membrane performance test

3.3.1. Humic acid removal

Figure 8 illustrates the permeate flux of the treated water as a function of humic acid concentrations. U4 provides the highest permeate flux for all different concentrations compared with U3 which provides the lowest permeate flux, that because U4 has PEG 3 wt% and PVC 14wt%, but U3 has PVC 15wt% and PEG 2wt%. Increasing the main polymer concentration especially when it has high molecular weight decreases the pores' size, also a low percentage of pore former makes low porosity and low pore size as shown in Table 2. U1 (blank membrane) provides a permeate flux of 65, 51, 40, and 26 L/m².h (LMH) for separation of various concentrations of humic

acid 0.05, 0.1, 0.2, and 1 g/l respectively. The pore former PEG did not add during U1 preparation so, the permeate flux is lower than U2 which has a pore former (PEG) in the polymeric solution during preparation. The fluxes of U2 were 72, 55, 45, and 29 L/m².h (LMH) for separation of various concentrations of humic acid 0.05, 0.1, 0.2 and 1 g/l respectively. The addition of nanoparticles Mn(acac)₃ during polymeric solution preparation increases the hydrophilicity of the membranes. The results indicate that U4 provides the highest flux compared with other membranes, where it has a nano-solution (NS) percentage 1%, this nano-solution consists of Mn(acac)₃ and acetonitrile, where Mn(acac)₃ is considered metal-organic complex material. It has metal ions make cluster coordination with one, two- or three-dimensional structure of organic molecules to form a tetragonal porous shape with the high surface area which leads to improve the performance of the membranes [49].

Decreasing in NS % leads to decrease in flux such as U5 (0.5% NS), U6 (0.2% NS). U7 has the highest percentage of NS 1.2% but it provides low flux compared with U4 that may be due to a decrease in porosity of this membrane due to an increase in NS%. Also, using 1wt% NS during membrane formation (U4) provides a fast interchange rate for solvent and non-solvent during the coagulation step for membrane formation, which produces successful uniform

nanoparticle on the membrane matrix, so U4 provides the best membrane performance compared with other membranes. However, U7 has aggregation problems of nano-particles, which leads to low homogeneity and high viscosity of the polymeric solution during the preparation step, so the prepared membrane U7 provides lower permeate flux compared with U4 (1 wt% NS) and U5 (0.5wt% NS) although U7 provides the lowest contact angle, which means high hydrophilic membrane but the aggregation problems of nanoparticle effect on the membrane performance [53].

Figure 9 illustrates the separation percentage as a function of different feed concentrations. The separation percentage increases with an increase in NS %. The separation percentage enhancement sequence was U4>U3>U7>U5>U6>U2>U1. The U1 provides the lowest separation percentage for all different feed concentrations compared with other membranes; therefore, that due to a weak selective layer, which reduces the separation percentage. The addition of NS% for all membranes improved the separation percentage which reached 99.9 %, 99.8%, 99.7%, and 99.5% for separation of various concentrations of humic acid 0.05, 0.1, 0.2, and 1 g/l respectively at using U4 and the separation percentage of all other membranes that the NS was used during preparation is over 98%.

Table 3
Infrared transmittance of prepared membranes resulted by FTIR test [42-54].

Beaks number	Wavenumber cm ⁻¹	Assignment	Type of vibration
1	404 cm ⁻¹ to 556 cm ⁻¹	Mn-O	Chain stretch Metal & actylacetionate
2	506 cm ⁻¹ to 632 cm ⁻¹	C - Cl	Chloride
3	722 cm ⁻¹	C- H	Alkene
4	970 cm ⁻¹ -1064 cm ⁻¹	C-N or C- O	Amines or Alchols
5	1622 to 1800 cm ⁻¹	C=O	Carbonyl group
6	1960 cm ⁻¹ to 2535 cm ⁻¹	C- H stretching	Alkane (stretch)
7	1427.9 to 1500 cm ⁻¹	CH ₂ Scissoring	Chain stretch PVC & Metal
8	1490 cm ⁻¹ to 1580 cm ⁻¹	CH ₂ bend	Chain stretch PVC & PET
9	2966 to 3544 cm ⁻¹	OH stretching	Hydroxyl group

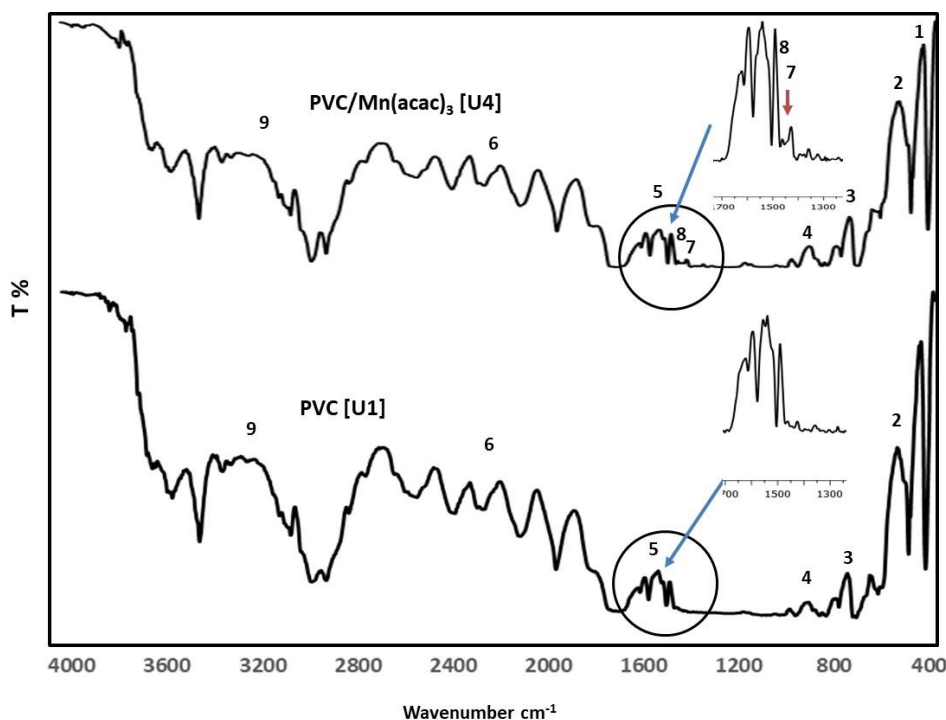


Fig. 7. FTIR spectra for prepared membranes U1(bare PVC), U4 (PVC/Mn(acac)₃).

3.3.2. Virus removal

Sewage wastewater contains many viruses the most common viruses are rotavirus, Aichi virus (AiV), and human bocavirus (HBoV) which are considered viral pathogens. The clear sewage wastewater sample was tested on the dead-end membrane filtration system. Table 3 illustrates the indication of viruses in the sewage wastewater before and after treatment by membranes. The results indicate that positive detection for the Aichi virus, human bocavirus, and rotavirus before the membrane. While after the U4 membrane (composed of 1wt% of Mn(acac)₃ solution) there is negative detection for all viruses, which means the U4 membrane separates all viruses from wastewater. U1 membrane (0% of Mn(acac)₃ solution) separates the only rotavirus maybe because this virus has a large size compared with other viruses, however, U1 depends on its membrane pores size to separate viruses by a sieving mechanism. While U4 has Mn(acac)₃ in its structure which exhibits complete removal of the viruses. Manganese atoms at the heart of Mn(acac)₃ knocking out the virus, that like a vaccine in the body, by oxidizing the amino acid residues of the proteins envelope on viruses [29,30].

Manganese organic complex compounds can break the protein structure of the viruses due to the high oxidation ability of these compounds with proteins, which can destroy the virus. However, the addition of these compounds in membrane fabrication can provide the disinfection membrane against any virus [31,32,46].

3.4. Membrane fouling test

Figure 10 illustrates that the membranes exhibit antifouling behavior, where the results indicate that washing of the membrane surface after using humic acid solution many times provides the ability to use membranes again. The results indicate that R_r was 72.8% for U1, 80.6% For U2, and 60.64% For U4. Irreversible resistance R_{ir} was 15.86% for U1, 4.76% U2, and 0.526% for U4. However, the FRR for U1 was 84.14 %, 95.25% for U2, and 99.47% for U4 as shown in Figure 11. It can be observed that the irreversible resistance of U4 was very low that makes this membrane super antifouling. The results indicate that U1 has the lowest antifouling properties according to the absence of polyethylene glycol and nano-solution. However, improving the antifouling properties of U2 was due to using polyethylene glycol, which enhances the hydrophilic properties of the membrane and pores interconnectivity [18-20]. Using Mn(acac)₃ nano-solution with PEG enhances

the membrane hydrophilicity and antifouling membrane surface as shown in U4, that because the negative charge and paramagnetic properties of Mn(acac)₃ can make electrostatic charge between the membrane surface and humic acid solution. Esfahani et al, studied the aggregation of humic acid removal by the ultrafiltration membrane and zeta potential of these aggregation. Zeta potential of humic acid aggregation was the negative charge from -16 mV to -36 mV [46,51]. According to that using the humic acid solution in our work provides electrostatic repulsion between membrane surface which has a negative charge due to using Mn(acac)₃ during membrane preparation [7,46]. According to that, U4 has too low irreversible resistance compared with other membranes, which means U4 is a super-antifouling membrane that can be used in wastewater treatment. These laboratory results are the nucleus for producing this type of membrane (PVC/Mn(acac)₃) on large scale to be applied in pilot units as ultrafiltration spiral wound modules or large flat sheet membranes to be used as a membrane for wastewater treatment. After the success of the pilot test. The membranes can be produced in the form of an industrial scale to be applied in the wastewater plants.

4. Conclusions

PVC/Mn(acac)₃ mixed matrix membranes were fabricated by phase inversion technique. Manganese acetylacetonate Mn(acac)₃ nanoparticles were prepared using a green chemistry technique to be used in membranes mixed matrix preparation. The optimum Nano-solution (NS%) percentage which was used during polymeric solution preparation was 1wt% in U4. It provides the best tensile strength of 221.7±0.05 MPa and elongation of 20.12±0.1 mm. U4 provides the highest permeate flux and removal percentage compared with other membranes. The addition of NS% for all membranes improved the hydrophilicity of membranes and reduced porosity, which leads to an improvement in the separation percentage. The virus removal was studied using U1 (blank PVC membrane) and U4 (PVC/Mn(acac)₃, 1wt% NS). U4 exhibits 100% removal of rotavirus, Aichi virus, and human bocavirus. The antifouling test was carried out between U1 (blank PVC), U2 (PVC/PEG without NS), and U4 (PVC/ Mn(acac)₃, 1wt% NS). U4 exhibits super-antifouling properties. From these results, the mixed matrix membrane U4 (PVC/ Mn(acac)₃, 1wt% NS) can be considered a fouling and virus resistance membrane.

Table 3

Indication of viruses in the sewage wastewater before and after treatment by membrane.

Virus type	Before membrane	After membrane		Removal %	
		U1	U4	U1	U4
human bocavirus	+ve	+ve	-ve	Less than the feed	100%
Aichi virus	+ve	+ve	-ve	Few amount	100%
rotavirus	+ve	-ve	-ve	100%	100%

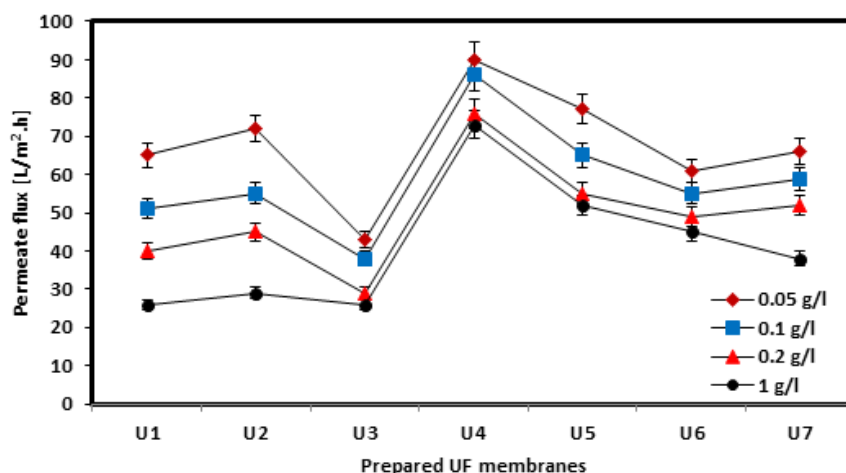


Fig. 8. Permeate flux of prepared UF PVC/Mn(acac)₃ membranes.

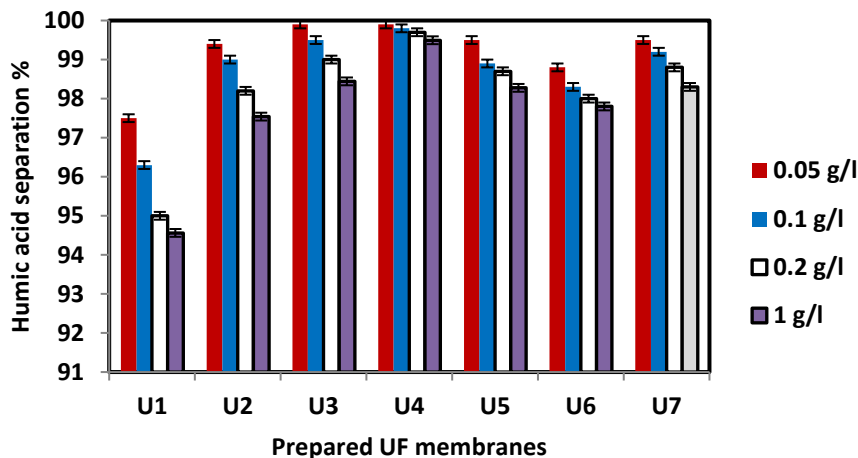


Fig. 9. Humic acid separation percentage using PVC/Mn(acac)₃ membranes.

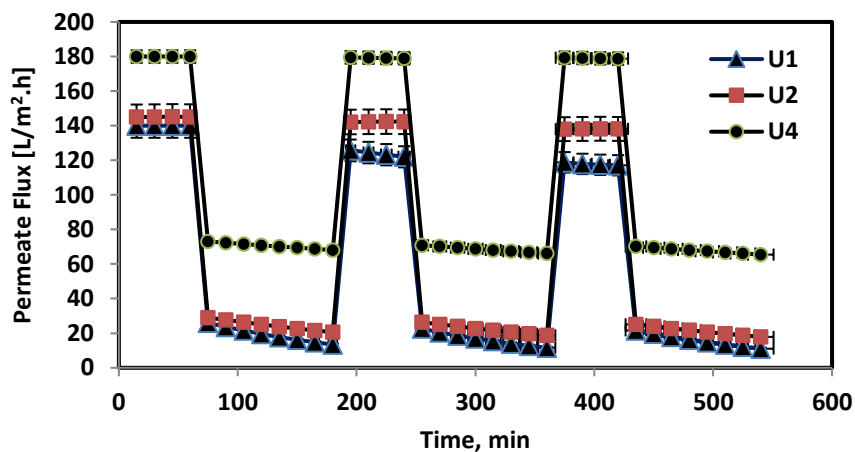


Fig. 10. Fouling test using prepared membranes U1, U2, and U4.

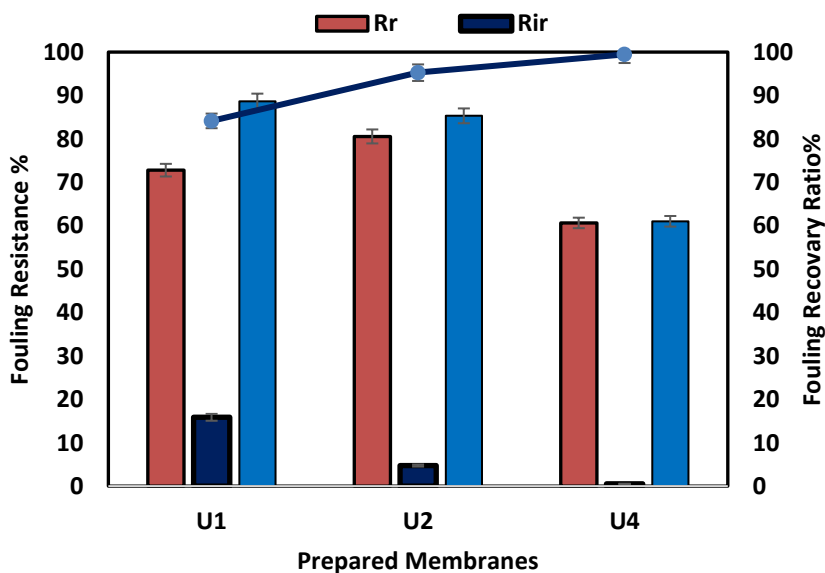


Fig. 11. Fouling resistance & FRR using prepared membranes U1, U2, and U4.

Acknowledgments

The authors would like to acknowledge the Science and Technological Development Fund (STDF), Egypt, and the Ministry of Science & Technology of the People's Republic of China due to their financial support and all facilities they offered to perform this work, through the Project No. (30431), Egypt-China Cooperation Program.

References

- [1] B. C. Liu, C. Chen, W. Zhang, J. Crittenden, Y. S. Chen, Low-cost antifouling PVC ultrafiltration membrane fabrication with Pluronic F 127: Effect of additives on properties and performance, *Desalination* 307 (2012) 26-33. <https://doi.org/10.1016/j.desal.2012.07.036>.
- [2] K. J. Howe, M. M. Clark, Fouling of microfiltration and ultrafiltration membranes by natural waters, *Environ Sci Technol* 36 (16) (2002) 3571-3576. DOI: 10.1021/es025587r.
- [3] Z. Yu, X. Liu, F. Zhao, X. Liang, Fabrication of a Low-Cost Nano-SiO₂/PVC Composite Ultrafiltration Membrane and its Antifouling Performance, *J. Appl. Polym. Sci.* 132 (2015) 41267. <https://doi.org/10.1002/app.41267>.
- [4] X. Z. Zhang, Y. S. Chen, A. H. Konsowa, X. S. Zhu, J. C. Crittenden, Evaluation of an innovative polyvinyl chloride (PVC) ultrafiltration membrane for wastewater treatment, *Sep. Purif. Technol.* 70 (2009) 71-78. <https://doi.org/10.1016/j.seppur.2009.08.019>
- [5] J. A. Xu, Z. L. Xu, Poly(vinyl chloride) (PVC) hollow fiber ultrafiltration membranes prepared from PVC/additives/solvent, *J. Membr. Sci.* 208 (2002) 203-212. [https://doi.org/10.1016/S0376-7388\(02\)00261-2](https://doi.org/10.1016/S0376-7388(02)00261-2)
- [6] R. Y. M. Huang, P. Shao, C. M. Burns, X. Feng, Sulfonation of poly(ether ether ketone)(PEEK): Kinetic study and characterization, *J. Appl. Polym. Sci.* 142 (2012) 2087. <https://doi.org/10.1002/app.2118>.
- [7] H. L. Liu, C. F. Xiao, Q. L. Huang, X. Y. Hu, Structure design and performance study on homogeneous-reinforced polyvinyl chloride hollow fiber membranes, *Desalination* 331 (2013) 35-45. <https://doi.org/10.1016/j.desal.2013.10.015>.
- [8] V. Kochkodan, N. Hilal, A comprehensive review on surface modified polymer membranes for biofouling mitigation, *Desalination* 356 (2015): 187-207. <https://doi.org/10.1016/j.desal.2014.09.015>
- [9] M. Reza kazemi, A. Dashti, H. R. Harami, N. Hajilari, Fouling-resistant membranes for water reuse, *Environ Chem Letters* 16 (2018) 715-763. <https://doi.org/10.1007/s10311-018-0717-8>.
- [10] M. Reza kazemi, A. Khajeh, M. Mesbah, Membrane filtration of wastewater from gas and oil production, *Environ Chem Letters* 16 (2018) 367-388. <https://doi.org/10.1007/s10311-015-0542-2>.
- [11] D. Rana, T. Matsuura, Surface Modifications for Antifouling Membranes, *Chem. Rev.* 110 (2010) 2448-2471. <https://doi.org/10.1021/cr800208y>.
- [12] P. P. Wang, J. Ma, Z.H. Wang, F. M. Shi, Q. L. Liu, Enhanced Separation Performance of PVDF/PVP-g-MMT Nanocomposite Ultrafiltration Membrane Based on the NVP-Grafted Polymerization Modification of Montmorillonite (MMT), *Langmuir* 28 (2012) 4776-4786. <https://doi.org/10.1021/la203494z>
- [13] M.P.González Muñoz, R. Navarro, I. Saucedo, M. Avila, P. Prádanos, L. Palacio, F. Martínez, A. Martín, A. Hernández, Hydrofluoric acid treatment for improved performance of a nanofiltration membrane, *Desalination* 191 (2006) 273-278. <https://doi.org/10.1016/j.desal.2005.06.040>
- [14] H. R. Lohokare, S. C. Kumbharkar, Y. S. Bhole, U. K. Kharul, Surface modification of polyacrylonitrile based ultrafiltration membrane, *J. Appl. Polym. Sci.* 101 (2006) 4378-4385. <https://doi.org/10.1002/app.23917>.
- [15] D. B. Mosqueda-Jimenez, R. M. Narbaitz, T. Matsuura, Effects of preparation conditions on the surface modification and performance of polyethersulfone ultrafiltration membranes, *J. Appl. Polym. Sci.* 99 (2006) 2978-2988. <https://doi.org/10.1002/app.22993>
- [16] J. Q. Meng, J. Q. Li, J. H. Zhang, Y. F. Ma, S. Ma, A novel controlled grafting chemistry fully regulated by light for membrane surface hydrophilization and functionalization, *J. Membr. Sci.* 455 (2014) 405-414. <https://doi.org/10.1016/j.memsci.2014.01.007>.
- [17] J. Huang, K. S. Zhang, K. Wang, Z. L. Xie, B. Ladewig, H. T. Wang, Fabrication of polyethersulfone-mesoporous silica nanocomposite ultrafiltration membranes with antifouling properties, *J. Membr. Sci.* 423 (2012) 362-370. <https://doi.org/10.1016/j.memsci.2012.08.029>.
- [18] J. Cai, X. L. Cao, Yi. Zhao, F.Y. Zhou, Z. Cui, Y. Wang, S. P. Sun, The establishment of high-performance anti-fouling nanofiltration membranes via cooperation of annular supramolecular Cucurbit[6]uril and dendritic polyamidoamine, *J. Membr. Sci.* 600 (2020) 117863. <https://doi.org/10.1016/j.memsci.2020.117863>.
- [19] S. Zhao, Z. Wang, J. X. Wang, S. B. Yang, S. C. Wang, PSf/PANI nanocomposite membrane prepared by in situ blending of PSf and PANI/NMP, *J. Membr. Sci.* 376 (2011) 83-95. <https://doi.org/10.1016/j.memsci.2011.04.008>.
- [20] J. N. Shen, C. C. Yu, H. M. Ruan, C. J. Gao, B. Van der Bruggen, Preparation and characterization of thin-film nanocomposite membranes embedded with poly(methyl methacrylate) hydrophobic modified multiwalled carbon nanotubes by interfacial polymerization, *J. Membr. Sci.* 442 (2013) 18-26. <https://doi.org/10.1016/j.memsci.2013.04.018>.
- [21] A. El-Gendi, H. Abdallah, A. Amin, S. K. Amin, Investigation of polyvinylchloride and cellulose acetate blend membranes for desalination, *J. Mol. Struct.* 1146 (2017) 14-22. <https://doi.org/10.1016/j.molstruc.2017.05.122>.
- [22] M. Delavar, G. Bakeri, M. Hossein, Fabrication of polycarbonate mixed matrix membranes containing hydrous manganese oxide and alumina nanoparticles for heavy metal decontamination: Characterization and comparative study, *Chem. Eng. Res. Des.* 120 (2017) 240-253. <https://doi.org/10.1016/j.cherd.2017.02.029>.
- [23] S. Pourjafar, A. Rahimpour, M. J. Jahanshahi, Synthesis and characterization of PVA/PES thin film composite nanofiltration membrane modified with TiO₂ nanoparticles for better performance and surface properties, *Ind. Eng. Chem.* 18 (2012) 1398-1405. <https://doi.org/10.1016/j.jiec.2012.01.041>.
- [24] Q. Q. Wang, X.T. Wang, Z.H. Wang, J. Huang, Y. J. Wang, PVDF membranes with simultaneously enhanced permeability and selectivity by breaking the trade off effect via atomic layer deposition of TiO₂, *J. Membr. Sci.* 442 (2013) 57-64. <https://doi.org/10.1016/j.memsci.2013.04.026>.
- [25] N. Maximous, G. Nakhla, W. Wan, K. Wong, Performance of a novel ZrO₂/PES membrane for wastewater filtration, *J. Membr. Sci.* 352 (2010) 222-230. <https://doi.org/10.1016/j.memsci.2010.02.021>.
- [26] A. L. Ahmad, M. A. Majid, B. S. Ooi, Functionalized PSf/SiO₂ nanocomposite membrane for oil-in-water emulsion separation, *Desalination* 268 (2011) 266-269. <https://doi.org/10.1016/j.desal.2010.10.017>.
- [27] H. A. Shawky, S. R. Chae, S. H. Lin, M. R. Wiesner, Synthesis and characterization of a carbon nanotube/polymer nanocomposite membrane for water treatment, *Desalination* 272(2011) 46-50. <https://doi.org/10.1016/j.desal.2010.12.051>.
- [28] Y. Mansourpanah, S. S. Madaeni, A. Rahimpour, M. Adeli, M. Y. Hashemi, M. R. Moradian, Fabrication new PES-based mixed matrix nanocomposite membranes using polycaprolactone modified carbon nanotubes as the additive: Property changes and morphological studies, *Desalination* 277 (2011) 171-177. <https://doi.org/10.1016/j.desal.2011.04.022>.
- [29] D. Weng, C. Lei, T. T. Wu, R. Sun, M. Shen, Y. Lu, Spontaneous and continuous anti-virus disinfection from nonstoichiometric perovskite-type lanthanum manganese oxide, *Pro. Nat. Sci. Mater.* 25 (2015) 191-196. <https://doi.org/10.1016/j.pnsc.2015.05.003>.
- [30] Y. Zuo, J. Li, J. Yi, Z. Wang, C. Chen, Determination of A-site deficiency in lanthanum manganite by XRD intensity ratio, *J. Solid State Chem.* 181(2008) 700-704. <https://doi.org/10.1016/j.jssc.2007.12.033>.
- [31] E. M. Rodríguez, J. L. Acero, L. Spool, J. Meriluoto, Oxidation of MC-LR and -RR with chlorine and potassium permanganate: toxicity of the reaction products, *Water Res.* 42 (2008) 1744-1752. DOI: 10.2166/wst.2008.460.
- [32] C. W. White, J. G. Martin, Chlorine Gas Inhalation Human Clinical Evidence of Toxicity and Experience in Animal Models, *Proc. Am. Thorac. Soc.* 7 (2010) 257-263. DOI: 10.1513/pats.201001-008SM.
- [33] E. Bouwman, R. van Gorkum, A study of new manganese complexes as potential driers for alkyd paints, *J. Coat. Technol. Res.* 4 (2007) 491-503. DOI 10.1007/s11998-007-9041-0.
- [34] S.N. Slabzhennikov, O. B. Ryabchenko, L.A. Kuarton, Distinctive and Regular Features of the IR Spectra of Transition Metal Tris(acetylacetonates), *Russ J. Coord Chem.* 34 (2008) 558-560. DOI: 10.1134/S1070328408070130.
- [35] M. Mahdavian, M. M. Attar, Electrochemical behaviour of some transition metal acetylacetonate complexes as corrosion inhibitors for mild steel, *Corros. Sci.* 51 (2009) 409-414. <https://doi.org/10.1016/j.corsci.2008.11.010>.
- [36] H. Abdallah, M. S. Shalaby, A. M. H. Shaban, Performance and Characterization for Blend Membrane of PES with Manganese (III) Acetylacetonate as Metalorganic Nanoparticles, *Int. J. Chem. Eng.* 2015 (2015) 1-9. <https://doi.org/10.1155/2015/896486>.
- [37] Q. Alsally, S. Algeborg, G. M. Alwan, S. Simone, A. Figoli, E. Drioli, Hollow Fiber Ultrafiltration Membranes from Poly(Vinyl Chloride): Preparation, Morphologies, and Properties, *Sep. Sci. Technol.* 46 (2011) 2199-2210. <https://doi.org/10.1080/01496395.2011.594845>
- [38] T. Jin, Z. Zhao, K. Chen, Preparation of a poly(vinyl chloride) ultrafiltration membrane through the combination of thermally induced phase separation and non-solvent-induced phase separation, *J. Appl. Polym. Sci.* 133 (2016) 42953. DOI: 10.1002/APP.42953.
- [39] L. Krishnamoorthy, P. M. Arif, R. Ahmedkhan, Separation of proteins from aqueous solution using cellulose acetate/poly (vinyl chloride) blend ultrafiltration membrane, *J Mater Sci* (2011) 46:2914-2921. DOI 10.1007/s10853-010-5166-0.
- [40] M. S. Shalaby, H. Abdallah, Preparation of manganese (III) acetylacetonate nanoparticles via an environmentally benign route, *Front. Chem. Sci. Eng.* 7 (2013) 329-337. DOI 10.1007/s11705-013-1339-0.
- [41] H. Abdallah, M. S. Shalaby, A. El-gendi, A. M. Shaban and B. K. Zhu, Effectiveness of a coagulation step and polyester support on blend polyvinylchloride membrane formation and performance, *J Polym Eng.* 39 (2019) 351-359. <https://doi.org/10.1515/poleng-2018-0387>.
- [42] E. Bagheripour, A. R. Moghadasi, S. M. Hosseini, Preparation and Characterization of PES-Blend-Sulfonated PVC Nanofiltration Membranes: Investigation of Polymers Blend Ratio, *Arab J Sci Eng* 41 (2016) 2545-2552. DOI 10.1007/s13369-016-2026-5.
- [43] S. Kang, A. Asatekin, M. Elimelech, A. M. Mayes, Protein antifouling mechanisms of PAN UF membranes incorporating PAN-g-PEO additive, *J. Membr. Sci.* 296 (2007) 42-50. DOI: 10.1016/J.MEMSCI.2007.03.012.
- [44] J. Peng, Y. Su, Q. Shi, W. Chen, Z. Jiang, Protein fouling resistant membrane

- prepared by amphiphilic pegylated polyethersulfone, *Bioresour. Technol.* 102 (2011) 2289–2295. <https://doi.org/10.1016/j.biortech.2010.10.045>.
- [45] D. Chen, J. Zhao, P. Zhang, S. Dai, Mechanochemical synthesis of metal–organic frameworks. *Polyhedron*. 162 (2019) 59–64. <https://doi.org/10.1016/j.poly.2019.01.024>.
- [46] M. R. Esfahani, H. A. Stretz, M. J.M. Wells, Abiotic reversible self-assembly of fulvic and humic acid aggregates in low electrolytic conductivity solutions by dynamic light scattering and zeta potential investigation, *Sci. Total Environ.* 537 (2015) 81–92. <https://doi.org/10.1016/j.scitotenv.2015.08.001>.
- [47] M. Razali, C. Didaskalou, J. F. Kim, M. Babaei, E. Drioli, Y. M. Lee, G. Szekely, Exploring and Exploiting the Effect of Solvent Treatment in Membrane Separations, *ACS Appl. Mater. Interfaces*. 9(2017)11279–11289. <https://doi.org/10.1021/acsami.7b01879>.
- [48] L.Y. Yu, Z. L. Xu, H. M. Shen, H. Yang, Enrichment of α -lactalbumin from diluted whey with polymeric ultrafiltration membranes, *J. Membr. Sci.* 337 (2009) 257–265. <https://doi.org/10.1016/j.memsci.2009.03.052>.
- [49] G. Arthanareeswarana, D. Mohan, M. Raajenthiren, Preparation, characterization and performance studies of ultrafiltration membranes with polymeric additive, *J Membr Sci* 350 (2010) 130–138. <https://doi.org/10.1016/j.memsci.2009.12.020>.
- [50] N. C. Wang, L. F. Fang, J. Wang, P. Zhang, W. B. Wang, C.E. Lin, L. Xiao, C. Chen, B. Zhao, H. Abdallah, H. Matsuyama, B.K. Zhu, pH-dependent property of carboxyl-based ultrafiltration membranes fabricated from poly (vinyl chloride-r-acrylic acid), *J. Appl. Polym. Sci.* 47068 (2018) 1–9. <https://doi.org/10.1002/app.47068>.
- [51] A. Tizchang, Y. Jafarzadeh, R. Yegani, E. Shokri, Polysulfone nanocomposite membrane embedded by silanized nano diamond for removal of humic acid from water, *J. Water Environ. Nanotechnol.* 4 (3) (2019) 213–226. doi 10.22090/JWENT.2019.03.004.
- [52] I. Diaz-Acosta, J. Baker, W. Cordes, P. Pulay, Calculated and experimental geometries and infrared spectra of metal tris-acetylacetonates: Vibrational spectroscopy as a probe of molecular structure for ionic complexes, Part ii. *Spectrochim Acta A Mol Biomol Spectrosc.* 59 (2003) 363–377. <https://doi.org/10.1021/jp0028599>.
- [53] T. S. Jamil, E. S. Mansor, Heba Abdallah, Ahmed M. Shaban, Eglal R. Souay, Novel anti fouling mixed matrix CeO₂/Ce₂O₁₂ nanofiltration membranes for heavy metal uptake, *J Environ Chem Eng.* 6 (2018) 3273–3282. <https://doi.org/10.1016/j.jece.2018.05.006>.
- [54] M. Tang, M. Liu, D. Wang, D. Shao, H. Wang, Z. Cui, X. Cao, Shi-Peng Sun, Precisely Patterned Nanostrand Surface of Cucurbituril[n]-Based Nanofiltration Membranes for Effective Alcohol-Water Condensation, *Nano Lett* 8 (2020) 2717–2723. doi: 10.1021/acs.nanolett.0c00344.